A Computationally Efficient, Transient-Pressure Solution for Inclined Wells

E. Ozkan, SPE, Colorado School of Mines, and **R. Raghavan,** SPE, Phillips Petroleum Co.

Summary

This work provides an efficient algorithm to compute transient pressure responses of inclined wells. The solution is derived in the Laplace domain and cast into computationally efficient forms for all inclination angles. The algorithm allows the computation of pressures and derivatives at the wellbore as well as at observation points. Short- and long-time approximations for the evaluation of pressure responses are also provided. The long-time approximation is used to derive a general pseudoskin expression that is applicable for all inclination angles. Example computations are presented in the forms of tables and figures to display the efficacy, accuracy, and the practical use of the algorithm.

Introduction

The central contribution of this work is to present a new solution to compute pressure distributions caused by directionally drilled (inclined or slanted) wells. This solution is presented in terms of the Laplace transformation. We present a computationally attractive scheme that may be used for inclinations from vertical to horizontal; this feature permits us to compute pressure distributions for partially penetrating or limited-entry and extended-reach wells. Thus, our contribution removes a restriction that is often noted in the literature regarding the Cinco *et al.*[1] solution (see Ref. 2). Results from our solution are compared with available solutions for vertical, inclined, and horizontal wells.

The mathematical model is identical to that considered by Cinco *et al.*[1] except that we work in terms of the Laplace transformation. We, however, present results for conditions not considered in Ref. 1 (high-angle and limited-entry wells). The advantage of working in terms of the Laplace transformation is that the extensions to the variable rate and wellbore storage and skin problems, the naturally fractured-reservoir formulation, and commingled-reservoir behavior may be readily handled. The focus of this work is on computational issues.

The specific contributions of this communication are as follows: We present a viable and tractable solution to compute pressure distributions. Alternate forms of the solution are presented to permit computations for all time ranges of interest. An expression for the pseudoskin function is derived. This expression is useful in obtaining long-time, fluid flow responses around an inclined well and should be suitable for calculating the productivity index and transmissibility modifiers in reservoir simulation models. We present results in tabular form so as to permit others to evaluate their own codes; we supplement the information documented by Cinco *et al.*[1] by concentrating on high-angle and limited-entry cases.

Mathematical Model

We consider the classic problem of the unsteady flow of a slightly compressible liquid to an inclined well in a reservoir that is infinite in its lateral extent. The top and bottom boundaries are impermeable. The well is assumed to be a line source and production may or may not take place over its entire length; that is, we examine limited-entry or partially penetrating wells. Two-dimensional anisotropy is considered; k_h and k_z represent the permeabilities in the horizontal and vertical directions, respectively. The pressure is uniform initially throughout the reservoir and equal to p_i. The inclination angle of the well, ψ, is measured from the positive z axis in the clockwise direction. **Fig. 1** presents a schematic of the system examined here.

We use the following dimensionless variables: The dimensionless pressure is defined by

$$p_D=\frac{k_h h}{141.2qB\mu}(p_i-p), \tag{1}$$

the dimensionless time by

$$t_D=\frac{0.0002637k_h}{\phi c_t \mu l^2}t, \tag{2}$$

the dimensionless distances by

$$r_D=\frac{r}{l}, \tag{3}$$

$$z_D=\frac{z}{l}\sqrt{\frac{k_h}{k_z}}, \tag{4}$$

$$h_D=\frac{h}{l}\sqrt{\frac{k_h}{k_z}}, \tag{5}$$

and the dimensionless well length and transformed well inclination angle are defined, respectively, by

$$h_{wD}=\frac{h_w}{l}\sqrt{\frac{k_h}{k_z}\cos^2\psi+\sin^2\psi}, \tag{6}$$

$$\psi'=\tan^{-1}\left(\sqrt{\frac{k_z}{k_h}}\tan\psi\right). \tag{7}$$

The definitions of h_{wD} and ψ' given in Eqs. 6 and 7 are a result of the transformation of the original anisotropic system into one that is isotropic (the coordinate transformation does not only scale distances but also rotates angles). Thus, for example, the effect of anisotropy appears to be a simple scale contraction for the formation thickness (h_D), whereas it is both a scale change (h_{wD}) and rotation of the angle (ψ') for the inclined well. In Eqs. 2–7, l is some characteristic length of the system and for the numerical results presented in this paper, it is chosen to be the wellbore radius r_w. The midpoint of the well is denoted by z_{wD}, which is also defined as in Eq. 4.

Following the lines discussed in Ref. 3, and using the dimensionless variables defined above, the dimensionless pressure solution for an inclined well in an infinite slab reservoir is given in the Laplace domain by

$$\overline{p_D}=\frac{1}{sh_{wD}\sin\psi'}\int_{-(h_{wD}/2)\sin\psi'}^{+(h_{wD}/2)\sin\psi'}\times\left[K_0(\sqrt{u}R_D)+2\sum_{n=1}^{\infty}K_0(\sqrt{u_n}R_D)\cos n\pi\frac{z_D-z_{wD}}{h_D}\times\cos n\pi\frac{z_{wD}+r'_D\cot g\,\psi'}{h_D}\right]dr'_D, \tag{8}$$

This paper (SPE 66206) was revised for publication from paper SPE 49085, prepared for presentation at the 1998 SPE Annual Technical Conference and Exhibition, New Orleans, 27–30 September. Original manuscript received for review 3 December 1998. Revised manuscript received 20 June 2000. Paper peer approved 30 June 2000.

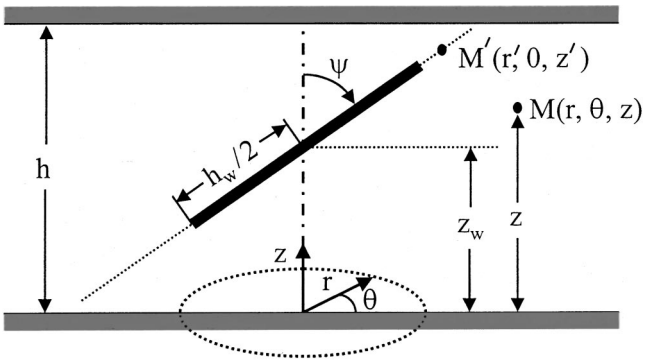

Fig. 1–Schematic of the inclined-well model.

where the overbar symbol denotes the Laplace transform and s is the Laplace transform parameter. We defined the following terms in Eq. 8:

$$R_D=\sqrt{(r_D\cos\theta-r'_D)^2+r_D^2\sin^2\theta}, \tag{9}$$

$$u=sf(s), \tag{10}$$

$$u_n=u+\frac{n^2\pi^2}{h_D^2}. \tag{11}$$

In Eq. 10, $f(s)$ is any one of the naturally fractured-reservoir-function formulations given in the literature.[3] For convenience, in this paper we restrict our attention to the homogeneous reservoir case where $f(s)=1$.

Although the solution given in Eq. 8 is complete, it is not particularly useful for numerical evaluations. In fact, although similar expressions have been known in the literature, they have not been used because of numerical difficulties.[4] Below, we re-cast Eq. 8 into alternate forms that make numerical evaluations possible for all time ranges. This constitutes the primary contribution of the present paper.

Computational Formulation

In order to re-cast Eq. 8 in computationally tractable forms, we follow the basic ideas presented in Refs. 3 and 5. Although the derivations may provide insight to the complexity of the computational issues and the problems one faces in computing pressure responses of inclined wells, because of length considerations, here we only present the final forms of the expressions.

For inclination angles different from zero, we may write Eq. 8 in the following form:

$$\overline{p}_D=\overline{p}_{Df}+\overline{F}. \tag{12}$$

The appropriate expressions for $\overline{p}_{Df}$ and $\overline{F}$ in Eq. 12 depend on the point where the pressure is computed and are given below:

If $|(z_D-z_{wD})\cos\psi'|\leq h_{wD}/2$, then

$$\overline{p}_{Df}=\frac{1}{s\sqrt{u}h_{wD}\sin\psi'}[Ki_{1c}(b_1,a,u)+Ki_{1c}(b_2,a,u)], \tag{13}$$

$$\overline{F}=\overline{F}_1-\overline{F}_2, \tag{14}$$

where

$$\overline{F}_1=\frac{2\pi}{sh_{wD}\sin\psi'}\sum_{n=1}^{\infty}\frac{1}{\sqrt{u+\alpha_n}}\cos n\pi\frac{z_{wD}+e}{h_D}\times\cos n\pi\frac{z_D}{h_D}\exp(-|r_D\sin\theta|\sqrt{u+\alpha_n}), \tag{15}$$

$$\overline{F}_2=\frac{2}{sh_{wD}\sin\psi'}\sum_{n=1}^{\infty}\frac{1}{\sqrt{u_n}}\times\cos n\pi\frac{z_D}{h_D}[I(b_1,\infty,-)+I(b_2,\infty,+)]. \tag{16}$$

If $(z_D-z_{wD})\cos\psi'\geq\frac{h_{wD}}{2}$, then

$$\overline{p}_{Df}=\frac{1}{s\sqrt{u}h_{wD}\sin\psi'}[Ki_{1c}(b_1,a,u)-Ki_{1c}(b_3,a,u)], \tag{17}$$

$$\overline{F}=\frac{2}{sh_{wD}\sin\psi'}\sum_{n=1}^{\infty}\frac{1}{\sqrt{u_n}}\times\cos n\pi\frac{z_D}{h_D}[I(b_3,\infty,-)-I(b_1,\infty,-)]. \tag{18}$$

If $(z_D-z_{wD})\cos\psi'\leq-\frac{h_{wD}}{2}$, then

$$\overline{p}_{Df}=\frac{1}{s\sqrt{u}h_{wD}\sin\psi'}[Ki_{1c}(b_2,a,u)-Ki_{1c}(b_4,a,u)], \tag{19}$$

$$\overline{F}=\frac{2}{sh_{wD}\sin\psi'}\sum_{n=1}^{\infty}\frac{1}{\sqrt{u_n}}\times\cos n\pi\frac{z_D}{h_D}[I(b_4,\infty,-)-I(b_2,\infty,-)]. \tag{20}$$

In Eqs. 13–20, we have used the following notations:

$$a=r_D\sin\theta, \tag{21}$$

$$b_1=r_D\cos\theta+\frac{h_{wD}}{2}\sin\psi', \tag{22}$$

$$b_2=\frac{h_{wD}}{2}\sin\psi'-r_D\cos\theta, \tag{23}$$

$$b_3=r_D\cos\theta-\frac{h_{wD}}{2}\sin\psi', \tag{24}$$

$$b_4=-\frac{h_{wD}}{2}\sin\psi'-r_D\cos\theta, \tag{25}$$

$$e=r_D\cos\theta\operatorname{cotg}\psi'=(z_D-z_{wD})\cos^2\psi', \tag{26}$$

$$\alpha_n=\frac{n^2\pi^2}{h_D^2\sin^2\psi'}, \tag{27}$$

$$Ki_{1c}(b,a,u)=\int_0^{b\sqrt{u}}K_0(\sqrt{\xi^2+a^2u})\,d\xi, \tag{28}$$

$$I(x_1,x_2,\pm)=\int_{x_1\sqrt{u_n}}^{x_2\sqrt{u_n}}K_0(\sqrt{\xi^2+a^2u_n})\times\cos n\pi\frac{z_{wD}+e\pm\frac{\xi}{\sqrt{u_n}}\operatorname{cotg}\psi'}{h_D}\,d\xi. \tag{29}$$

The expressions given above are general to compute pressure responses at the wellbore and observation points. Except for $\overline{F}_1$ defined in Eq. 15, the computations are straightforward provided that an appropriate integration algorithm is used. We have found that the Chebyshev polynomials provide an efficient and accurate

integration procedure for these computations. It is also useful to use the following transformation before evaluating the improper integrals appearing in Eqs. 16, 18, and 20:

$$\int_{x=a}^{x=b} f(x)\mathrm{d}x = \int_{t=0}^{t=\exp(-a)} f(-\ln t)\,\frac{\mathrm{d}t}{t}. \tag{30}$$

For the evaluation of $\overline{F}_1$ given in Eq. 15, we present two expressions that should be used for the small and large values of time (that is, for large and small values of the Laplace transform variable s). For small times, we may use the following expression to compute Eq. 15:

$$\begin{aligned}\overline{F}_1 = {} & \frac{h_D}{s h_{wD}} \sum_{n=-\infty}^{\infty} \\ & \times \{K_0[\sqrt{(z_D - z_{wD} - e - 2nh_D)^2 \sin^2\psi' + r_D^2 \sin^2\theta}\sqrt{u}] \\ & + K_0[\sqrt{(z_D + z_{wD} + e - 2nh_D)^2 \sin^2\psi' + r_D^2 \sin^2\theta}\sqrt{u}]\} \\ & - \frac{\pi}{s\sqrt{u} h_{wD} \sin\psi'} \exp(-|r_D \sin\theta|\sqrt{u}).\end{aligned} \tag{31}$$

In deriving Eq. 31, we have used the following relation given in Refs. 3 and 5:

$$\begin{aligned}\sum_{n=1}^{\infty} & \frac{\cos n\pi z_1 \cos n\pi z_2}{\epsilon_n} \exp(-\epsilon_n y) \\ & = \frac{z_e}{2\pi} \sum_{n=-\infty}^{\infty} \{K_0[\sqrt{(z_1 - z_2 - 2n)^2 z_e^2 + y^2}\sqrt{u + a^2}] \\ & + K_0[\sqrt{(z_1 + z_2 - 2n)^2 z_e^2 + y^2}\sqrt{u + a^2}]\} \\ & - \frac{\exp(-\sqrt{u + a^2}\,y)}{2\sqrt{u + a^2}},\end{aligned} \tag{32}$$

where

$$\epsilon_n = \sqrt{u + n^2\pi^2/z_e^2 + a^2}. \tag{33}$$

For large times, we may use the following expression to compute $\overline{F}_1$:

$$\begin{aligned}\overline{F}_1 = {} & \frac{2\pi}{s h_{wD} \sin\psi'} \sum_{n=1}^{\infty} \cos n\pi \frac{z_{D1}}{h_D} \\ & \times \cos n\pi \frac{z_{D2}}{h_D} \left[\frac{\exp(-|r_D \sin\theta|\sqrt{u + \alpha_n})}{\sqrt{u + \alpha_n}} \right. \\ & \left. - \frac{\exp(-|r_D \sin\theta|\sqrt{\alpha_n})}{\sqrt{\alpha_n}} \right] \\ & - \frac{h_D}{2s h_{wD}} \{\ln[1 - 2\exp(-\lambda)\cos\pi(z_{wD} + z_D + e) \\ & + \exp(-2\lambda)] + \ln[1 - 2\exp(-\lambda)\cos\pi(z_{wD} - z_D + e) \\ & + \exp(-2\lambda)]\},\end{aligned} \tag{34}$$

where

$$\lambda = \frac{\pi r_D \sin\theta}{h_D \sin\psi'}, \tag{35}$$

$$z_{D1} = \frac{z_{wD} + r_D \cos\theta \operatorname{cotg}\psi'}{h_D}, \tag{36}$$

and

$$z_{D2} = \frac{z_D}{h_D}. \tag{37}$$

We have used the following relation given in Ref. 3 to obtain the alternate form of Eq. 15 given in Eq. 34:

$$\begin{aligned}\sum_{n=1}^{\infty} & \frac{\cos n\pi z}{\epsilon_n} \exp(-\epsilon_n y) \\ & = \sum_{n=1}^{\infty} \cos n\pi z \left[\frac{\exp(-\epsilon_n y)}{\epsilon_n} - \frac{\exp(-n\pi y/z_e)}{n\pi/z_e} \right] \\ & - \frac{z_e}{2\pi} \ln[1 - 2\exp(-\pi y/z_e)\cos\pi z + \exp(-2\pi y/z_e)].\end{aligned} \tag{38}$$

The computational formulations of the inclined-well solution given above have not been reported previously. The lack of such formulations has been the major obstacle for computing the inclined-well responses in the Laplace transform domain and obtaining the results for large inclination angles.

We must note that Eq. 8 cannot be numerically evaluated for vertical wells. It is, however, possible to obtain the following limiting form of Eq. 8 as $\psi' \to 0°$:

$$\begin{aligned}\overline{p}_D = {} & \frac{1}{s} K_0(\sqrt{u} r_D) + \frac{4h_D}{\pi s h_{wD}} \sum_{n=1}^{\infty} \frac{1}{n} K_0(\sqrt{u_n} r_D) \\ & \times \cos n\pi \frac{z_D}{h_D} \cos n\pi \frac{z_{wD}}{h_D} \sin n\pi \frac{h_{wD}}{2h_D}.\end{aligned} \tag{39}$$

This expression is the same as that given in Ref. 6 for partially penetrating vertical wells and poses no computational difficulties.

Asymptotic Approximations

In this study, we have also derived the limiting forms of the solution given in Eq. 8 to obtain approximations to the short- and long-time wellbore pressure responses of inclined wells. Again, because of length considerations, we do not present the derivations of these approximations here. The final form of the approximations are given below:

If $\psi' \neq 0°$, then for early times,

$$p_D = -\frac{\beta h_D}{4h_{wD}} Ei\left[-\frac{(z_D - z_{wD} - e)^2 \sin^2\psi' + r_D^2 \sin^2\theta}{4t_D} \right], \tag{40}$$

where

$$\beta = \begin{cases} 2 & \text{for } |z_D - z_{wD}|\cos\psi' < h_{wD}/2 \\ 1 & \text{for } |z_D - z_{wD}|\cos\psi' = h_{wD}/2, \\ 0 & \text{for } |z_D - z_{wD}|\cos\psi' > h_{wD}/2 \end{cases} \tag{41}$$

and for late times

$$\begin{aligned}p_D = {} & \frac{1}{2}(\ln t_D + 0.80907) + 1 + \frac{2}{h_{wD} \sin\psi'} \\ & \times \sigma\left(r_D \cos\theta, r_D \sin\theta, -\frac{h_{wD}}{2}\sin\psi', \frac{h_{wD}}{2}\sin\psi' \right) + \hat{F},\end{aligned} \tag{42}$$

where

$$\begin{aligned}\sigma(x,y,a,b) = {} & \frac{1}{4}\left\{ (x - b)\ln[(x - b)^2 + y^2] \right. \\ & - (x - a)\ln[(x - a)^2 + y^2] \\ & \left. - \frac{y}{2}\left(\tan^{-1}\frac{x - a}{y} - \tan^{-1}\frac{x - b}{y} \right) \right\},\end{aligned} \tag{43}$$

$$\hat{F}=\begin{cases}\hat{F}_1-\hat{F}_2 & \text{for} \quad |(z_D-z_{wD})\cos\psi'|\leq h_{wD}/2\\ \hat{F}_a & \text{for} \quad (z_D-z_{wD})\cos\psi'\geq h_{wD}/2\\ \hat{F}_b & \text{for} \quad (z_D-z_{wD})\cos\psi'\leq -h_{wD}/2,\end{cases} \tag{44}$$

$$\hat{F}_1=-\frac{h_D}{2h_{wD}}\{\ln[1-2\exp(-p)\cos\pi(z_D+z_{wD}+e)+\exp(-2p)]+\ln[1-2\exp(-p)\cos\pi(z_D-z_{wD}-e)+\exp(-2p)]\}, \tag{45}$$

$$\hat{F}_2=\frac{2h_D}{\pi h_{wD}\sin\psi'}\sum_{n=1}^{\infty}\frac{1}{n}\cos n\pi\frac{z_D}{h_D}[I_0(b_1,\infty,-)+I_0(b_2,\infty,+)], \tag{46}$$

$$\hat{F}_a=\frac{2h_D}{\pi h_{wD}\sin\psi'}\sum_{n=1}^{\infty}\frac{1}{n}\cos n\pi\frac{z_D}{h_D}[I_0(b_3,\infty,-)-I_0(b_1,\infty,-)], \tag{47}$$

$$\hat{F}_b=\frac{2}{\pi h_{wD}\sin\psi'}\sum_{n=1}^{\infty}\frac{1}{n}\cos n\pi\frac{z_D}{h_D}[I_0(b_4,\infty,-)-I_0(b_2,\infty,-)]. \tag{48}$$

In Eqs. 46–48,

$$I_0(x_1,x_2,\pm)=\int_{x_1}^{x_2}K_0\left(\sqrt{\xi^2+a^2\frac{n^2\pi^2}{h_D^2}}\right)\times\cos n\pi\frac{z_{wD}+e\pm\frac{\xi h_D}{n\pi}\operatorname{cotg}\psi'}{h_D}\,d\xi. \tag{49}$$

If $\psi'=0°$, then for early times,

$$p_D=-\frac{\beta h_D}{4h_{wD}}Ei\left(-\frac{r_D^2}{4t_D}\right), \tag{50}$$

and for late times,

$$p_D=\frac{1}{2}\left(\ln\frac{t_D}{r_D^2}+0.80907\right)+\frac{4h_D}{\pi h_{wD}}\sum_{n=1}^{\infty}\frac{1}{n}K_0\left(\frac{n\pi}{h_D}r_D\right)\times\cos n\pi\frac{z_D}{h_D}\cos n\pi\frac{z_{wD}}{h_D}\sin n\pi\frac{h_{wD}}{2h_D}. \tag{51}$$

Computation of Wellbore Pressures

As we noted before, the above formulation of the inclined-well solution assumes a line-source well. Assuming an infinite-conductivity wellbore, Cinco[7] obtained the r,θ,z coordinates of the equivalent-pressure point at which the wellbore pressure responses of fully penetrating, inclined wells may be computed. We have modified Cinco's equivalent-pressure point for all well penetrations and obtained the following coordinates:

$$r_D=\sqrt{1+0.09h_{wD}^2\sin^2\psi'}, \tag{52}$$

$$\theta=\cos^{-1}\left(\frac{0.3h_{wD}\sin\psi'}{r_D}\right), \tag{53}$$

and

$$z_D=z_{wD}\pm 0.3h_{wD}\cos\psi', \tag{54}$$

where the plus and minus signs correspond, respectively, to the well locations in the upper and lower halves of the formation.

It should be emphasized that the focus of the present paper is to develop a computationally efficient, transient-pressure solution for inclined wells. The rigorous definition of the equivalent-pressure point and the procedures to compute the infinite-conductivity responses are not in the scope of our work. We have used the above coordinates of the equivalent-pressure point mainly to compare our results with the data available in the literature. We must note, however, that the above coordinates provided very good agreement with the other published data obtained by using an equivalent-pressure point approach.[1,8,9] When we compared our results with the data from rigorous infinite-conductivity computations,[7,8,10,11] the agreement was satisfactory.

Pseudoskin Factor

In the literature, several pseudoskin expressions for inclined wells have been presented.[1,2,10,12-14] The pseudoskin function presented by Cinco *et al.*[1] is one of the most commonly used expressions but it is limited to slant angles less than or equal to 75° (see also Ref. 8). The other expressions are based on approximate analytical solutions or simulation results and are better than that of Cinco *et al.* only if they provide results for inclination angles larger than 75°.

The long-time approximation for the pressure distribution derived in this work leads to a new pseudoskin expression for inclined wells. For $\psi'\neq 0$, this new expression is as follows:

$$S_g=1+\frac{2}{h_{wD}\sin\psi'}\sigma\left(r_D\cos\theta, r_D\sin\theta, -\frac{h_{wD}}{2}\sin\psi', \frac{h_{wD}}{2}\sin\psi'\right)+\hat{F}_1-\hat{F}_2, \tag{55}$$

where σ, $\hat{F}_1$, and $\hat{F}_2$ are given, respectively, by Eqs. 43, 45, and 46. The values of r_D, θ, and z_D should be computed from Eqs. 52–54.

Analytically, it can be shown that $\hat{F}_2$ is negligibly small compared with $\hat{F}_1$ and within 1% of $\hat{F}_1$ when

$$\frac{h_{wD}}{h_D}\geq\frac{2.3}{\sin\psi'}. \tag{56}$$

Our computations indicate that for fully penetrating, inclined wells, the contribution of $\hat{F}_2$ may be ignored with less than 5% error if $\psi'\geq 50°$ and with less than 1% error if $\psi'\geq 65°$. The condition given by Eq. 56 also indicates that for many extended-reach and horizontal wells, the pseudoskin factor may be simplified by dropping the $\hat{F}_2$ term in Eq. 55. The pseudoskin factor given above may be used to obtain expressions for stabilized flow periods, to compute the productivity indices of inclined wells, and for the simulation of production with inclined wells.

For completeness, we again note that for vertical wells ($\psi'=0°$), the expression given in Eq. 55 should be evaluated asymptotically. In this case, we obtain the following expression, which was also derived in Ref. 6:

$$S_g=\frac{4h_D}{\pi h_{wD}}\sum_{n=1}^{\infty}\frac{1}{n}K_0\left(\frac{n\pi}{h_D}\right)\cos n\pi\frac{z_D}{h_D}\cos n\pi\frac{z_{wD}}{h_D}\sin n\pi\frac{h_{wD}}{2h_D}. \tag{57}$$

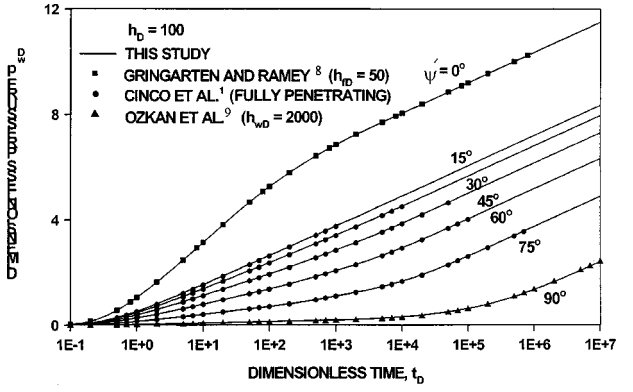

Fig. 2–Comparison of the results with the published solutions, $h_D=100$.

TABLE 1– DIMENSIONLESS WELLBORE PRESSURES OF FULLY PENETRATING INCLINED WELLS, $h_D=100$

	p_{wD}				
t_D	$\psi'=15°$	$\psi'=45°$	$\psi'=75°$	$\psi'=85°$	$\psi'=89°$
1×10	1.5148	1.1089	0.4058	0.1367	0.0274
2×10	1.8573	1.3493	0.4939	0.1663	0.0333
5×10	2.2827	1.6712	0.6115	0.2060	0.0412
7×10	2.4461	1.7916	0.6550	0.2206	0.0442
1×10^2	2.6194	1.9211	0.7015	0.2362	0.0473
2×10^2	2.9516	2.1842	0.7981	0.2684	0.0537
5×10^2	3.4193	2.5507	0.9529	0.3195	0.0640
7×10^2	3.5524	2.6877	1.0183	0.3419	0.0684
1×10^3	3.7168	2.8336	1.0910	0.3671	0.0735
2×10^3	4.0968	3.1228	1.2372	0.4205	0.0842
5×10^3	4.5579	3.5291	1.4507	0.5135	0.1011
7×10^3	4.7148	3.6859	1.5433	0.5163	0.1113
1×10^4	4.8820	3.8554	1.6529	0.5583	0.1204
2×10^4	5.2287	4.1915	1.9004	0.7111	0.1451
5×10^4	5.6870	4.6433	2.2853	0.9186	0.1959
7×10^4	5.8552	4.8103	2.4381	1.0129	0.2212
1×10^5	6.0334	4.9877	2.6045	1.1248	0.2550
2×10^5	6.3799	5.3332	2.9367	1.3764	0.1950
5×10^5	6.8380	5.7907	3.3860	1.7650	0.4807
7×10^5	7.0062	5.9588	3.5525	1.9187	0.5491
1×10^6	7.1846	6.1371	3.7296	2.0857	0.6311

TABLE 2– LOGARITHMIC DERIVATIVES OF WELLBORE PRESSURES OF FULLY PENETRATING INCLINED WELLS, $h_D=100$

	p'_{wD}				
t_D	$\psi'=30°$	$\psi'=45°$	$\psi'=75°$	$\psi'=85°$	$\psi'=89°$
1×10	0.4223	0.3444	0.1261	0.0424	0.0085
2×10	0.4286	0.3487	0.1277	0.0430	0.0086
5×10	0.4381	0.3527	0.1288	0.0434	0.0087
7×10	0.4407	0.3592	0.1296	0.0436	0.0087
1×10^2	0.4427	0.3684	0.1324	0.0444	0.0089
2×10^2	0.4528	0.3901	0.1491	0.0495	0.0099
5×10^2	0.4590	0.4069	0.1832	0.0619	0.0126
7×10^2	0.4613	0.4086	0.1938	0.0679	0.0137
1×10^3	0.4644	0.4109	0.2034	0.0731	0.0146
2×10^3	0.4689	0.4257	0.2203	0.0821	0.0164
5×10^3	0.4882	0.4606	0.2627	0.1007	0.0218
7×10^3	0.4901	0.4713	0.2879	0.1250	0.0301
1×10^4	0.4924	0.4798	0.3183	0.1441	0.0305
2×10^4	0.4964	0.4896	0.3799	0.1886	0.0438
5×10^4	0.4985	0.4955	0.4449	0.2625	0.0692
7×10^4	0.4989	0.4968	0.4613	0.2933	0.0818
1×10^5	0.4993	0.4977	0.4714	0.3268	0.0999
2×10^5	0.4996	0.4989	0.4851	0.3888	0.1315
5×10^5	0.4999	0.4996	0.4938	0.4504	0.1913
7×10^5	0.4999	0.4997	0.4956	0.4656	0.2159
1×10^6	0.5000	0.4998	0.4969	0.4778	0.2447

We have checked the pseudoskin factors computed by Eqs. 55 and 57 with those computed from the late-time pressure values and obtained excellent agreement.

Discussion of Results

Here, we present some results to show the accuracy, efficacy, and the practical use of the algorithm presented above. We first compare our results with those published in the literature. We then present some results in tabular form so as to permit others to evaluate their own codes. These results also complement the data presented by Cinco *et al.*[1] by considering high-angle and limited-entry cases. We also present graphical information on the pressure and derivative behavior and the pseudoskin factor of inclined wells.

TABLE 3– DIMENSIONLESS WELLBORE PRESSURES OF HIGHLY INCLINED, FULLY PENETRATING WELLS, $h_D=100$

	p_{wD}					
t_D	$\psi'=77°$	$\psi'=80°$	$\psi'=82°$	$\psi'=85°$	$\psi'=87°$	$\psi'=89°$
1×10	0.3527	0.2722	0.2182	0.1367	0.0823	0.0274
2×10	0.4293	0.3313	0.2656	0.1663	0.1000	0.0333
5×10	0.5315	0.4103	0.3288	0.2060	0.1238	0.0412
7×10	0.5692	0.4394	0.3521	0.2206	0.1326	0.0442
1×10^2	0.6096	0.4705	0.3771	0.2362	0.1420	0.0473
2×10^2	0.6933	0.5349	0.4286	0.2684	0.1613	0.0537
5×10^2	0.8275	0.6380	0.5110	0.3195	0.1921	0.0640
7×10^2	0.8848	0.6823	0.5464	0.3419	0.2054	0.0684
1×10^3	0.9490	0.7325	0.5867	0.3671	0.2205	0.0735
2×10^3	1.0799	0.8372	0.6717	0.4205	0.2526	0.0842
5×10^3	1.2725	0.9953	0.8035	0.5135	0.3040	0.1011
7×10^3	1.3561	1.0645	0.8621	0.5163	0.3282	0.1113
1×10^4	1.4555	1.1470	0.9323	0.5583	0.3585	0.1204
2×10^4	1.6837	1.3396	1.0971	0.7111	0.4344	0.1451
5×10^4	2.0496	1.6639	1.3824	0.9186	0.5763	0.1959
7×10^4	2.1977	1.8008	1.5069	1.0129	0.6422	0.2212
1×10^5	2.3603	1.9541	1.6492	1.1248	0.7212	0.2550
2×10^5	2.6879	2.2694	1.9494	1.3764	0.9060	0.1950
5×10^5	3.1342	2.7077	2.3772	1.7650	1.2199	0.4807
7×10^5	3.3002	2.8721	2.5394	1.9187	1.3536	0.5491
1×10^6	3.4768	3.0475	2.7132	2.0857	1.5041	0.6311

TABLE 4– DIMENSIONLESS WELLBORE PRESSURES OF HIGHLY INCLINED, FULLY PENETRATING WELLS, $h_D = 200$

	p_{wD}					
t_D	$\psi' = 77°$	$\psi' = 80°$	$\psi' = 82°$	$\psi' = 85°$	$\psi' = 87°$	$\psi' = 89°$
1×10	0.3527	0.2724	0.2183	0.1370	0.0825	0.0273
2×10	0.4293	0.3315	0.2657	0.1666	0.1003	0.0334
5×10	0.5315	0.4104	0.3290	0.2061	0.1239	0.0415
7×10	0.5692	0.4395	0.3523	0.2208	0.1327	0.0445
1×10^2	0.6092	0.4703	0.3770	0.2363	0.1420	0.0476
2×10^2	0.6871	0.5304	0.4252	0.2664	0.1601	0.0537
5×10^2	0.7914	0.6109	0.4896	0.3067	0.1843	0.0616
7×10^2	0.8322	0.6423	0.5147	0.3224	0.1937	0.0647
1×10^3	0.8790	0.6782	0.5434	0.3404	0.2045	0.0683
2×10^3	0.9835	0.7585	0.6076	0.3804	0.2285	0.0763
5×10^3	1.1465	0.8858	0.7098	0.4443	0.2668	0.0891
7×10^3	1.2102	0.9369	0.7513	0.4704	0.2825	0.0943
1×10^4	1.2798	0.9935	0.7978	0.4998	0.3002	0.1002
2×10^4	1.4286	1.1159	0.9002	0.5667	0.3404	0.1136
5×10^4	1.6800	1.3247	1.0777	0.6892	0.4166	0.1391
7×10^4	1.7923	1.4195	1.1589	0.7468	0.4542	0.1517
1×10^5	1.9228	1.5319	1.2558	0.8162	0.5006	0.1677
2×10^5	2.2056	1.7845	1.4790	0.9793	0.6127	0.2082
5×10^5	2.6204	2.1739	1.8395	1.2617	0.8124	0.2884
7×10^5	2.7799	2.3278	1.9862	1.3853	0.9033	0.3277
1×10^6	2.9516	2.4950	2.1478	1.5267	1.0114	0.3763
2×10^6	3.2902	2.8283	2.4739	1.8257	1.2562	0.4929
5×10^6	3.7436	3.2782	2.9193	2.2526	1.6384	0.7001
7×10^6	3.9109	3.4449	3.0851	2.4147	1.7906	0.7943
1×10^7	4.0885	3.6220	3.2616	2.5883	1.9565	0.9060

TABLE 5– DIMENSIONLESS WELLBORE PRESSURES OF HIGHLY INCLINED, FULLY PENETRATING WELLS, $h_D = 500$

	p_{wD}					
t_D	$\psi' = 77°$	$\psi' = 80°$	$\psi' = 82°$	$\psi' = 85°$	$\psi' = 87°$	$\psi' = 89°$
1×10	0.3531	0.2727	0.2187	0.1369	0.0821	0.0272
2×10	0.4295	0.3317	0.2660	0.1667	0.1000	0.0332
5×10	0.5317	0.4105	0.3291	0.2063	0.1240	0.0411
7×10	0.5694	0.4396	0.3524	0.2209	0.1328	0.0440
1×10^2	0.6094	0.4705	0.3772	0.2363	0.1421	0.0472
2×10^2	0.6873	0.5306	0.4253	0.2664	0.1602	0.0534
5×10^2	0.7902	0.6101	0.4890	0.3063	0.1840	0.0616
7×10^2	0.8281	0.6393	0.5124	0.3210	0.1928	0.0645
1×10^3	0.8682	0.6703	0.5373	0.3366	0.2022	0.0677
2×10^3	0.9462	0.7305	0.5855	0.3668	0.2203	0.0736
5×10^3	1.0555	0.8146	0.6528	0.4089	0.2456	0.0819
7×10^3	1.1011	0.8496	0.6808	0.4263	0.2560	0.0854
1×10^4	1.1541	0.8903	0.7133	0.4466	0.2682	0.0895
2×10^4	1.2708	0.9805	0.7855	0.4917	0.2953	0.0985
5×10^4	1.4423	1.1171	0.8961	0.5611	0.3369	0.1124
7×10^4	1.5089	1.1714	0.9409	0.5896	0.3540	0.1181
1×10^5	1.5842	1.2333	0.9926	0.6232	0.3742	0.1248
2×10^5	1.7543	1.3740	1.1117	0.7036	0.4232	0.1412
5×10^5	2.0461	1.6194	1.3215	0.8517	0.5187	0.1733
7×10^5	2.1729	1.7295	1.4168	0.9202	0.5648	0.1893
1×10^6	2.3173	1.8578	1.5298	1.0023	0.6212	0.2096
2×10^6	2.6204	2.1372	1.7834	1.1940	0.7549	0.2608
5×10^6	3.0503	2.5493	2.1737	1.5170	0.9903	0.3610
7×10^6	3.2129	2.7082	2.3278	1.6535	1.0963	0.4092
1×10^7	3.3870	2.8794	2.4952	1.8064	1.2206	0.4679

TABLE 6– DIMENSIONLESS WELLBORE PRESSURES OF HIGHLY INCLINED, FULLY PENETRATING WELLS, h_D=1,000

	p_{wD}					
t_D	$\psi'=77°$	$\psi'=80°$	$\psi'=82°$	$\psi'=85°$	$\psi'=87°$	$\psi'=89°$
1×10	0.3531	0.2726	0.2184	0.1366	0.0819	0.0272
2×10	0.4298	0.3318	0.2659	0.1664	0.0998	0.0332
5×10	0.5319	0.4107	0.3293	0.2062	0.1237	0.0411
7×10	0.5695	0.4398	0.3526	0.2209	0.1325	0.0440
1×10^2	0.6095	0.4706	0.3773	0.2364	0.1419	0.0471
2×10^2	0.6873	0.5306	0.4253	0.2666	0.1601	0.0531
5×10^2	0.7903	0.6101	0.4890	0.3063	0.1841	0.0612
7×10^2	0.8281	0.6393	0.5124	0.3210	0.1929	0.0642
1×10^3	0.8682	0.6703	0.5372	0.3365	0.2022	0.0674
2×10^3	0.9462	0.7304	0.5855	0.3667	0.2202	0.0736
5×10^3	1.0492	0.8100	0.6492	0.4066	0.2442	0.0816
7×10^3	1.0871	0.8392	0.6727	0.4213	0.2530	0.0845
1×10^4	1.1277	0.8705	0.6977	0.4370	0.2625	0.0876
2×10^4	1.2115	0.9350	0.7493	0.4692	0.2818	0.0940
5×10^4	1.3458	1.0381	0.8317	0.5207	0.3127	0.1043
7×10^4	1.4031	1.0825	0.8672	0.5428	0.3259	0.1087
1×10^5	1.4674	1.1327	0.9075	0.5680	0.3411	0.1138
2×10^5	1.5983	1.2374	0.9925	0.6214	0.3731	0.1245
5×10^5	1.7909	1.3956	1.1244	0.7069	0.4245	0.1416
7×10^5	1.8745	1.4647	1.1829	0.7466	0.4487	0.1496
1×10^6	1.9739	1.5472	1.2531	0.7952	0.4790	0.1597
2×10^6	2.2021	1.7398	1.4179	0.9120	0.5549	0.1854
5×10^6	2.5679	2.0642	1.7032	1.1196	0.6968	0.2362
7×10^6	2.7161	2.2011	1.8277	1.2139	0.7627	0.2616
1×10^7	2.8787	2.3543	1.9700	1.3258	0.8418	0.2934
2×10^7	3.2063	2.6696	2.2702	1.5774	1.0265	0.3730
5×10^7	3.6526	3.1080	2.6980	1.9660	1.3404	0.5209
7×10^7	3.8185	3.2723	2.8602	2.1196	1.4742	0.5893
1×10^8	3.9951	3.4477	3.0340	2.2867	1.6247	0.6713
2×10^8	4.3397	3.7909	3.3752	2.6198	1.9364	0.8626
5×10^8	4.7966	4.2469	3.8301	3.0696	2.3722	1.1853
7×10^8	4.9646	4.4148	3.9977	3.2362	2.5361	1.3217
1×10^9	5.1428	4.5928	4.1756	3.4134	2.7111	1.4745

Fig. 2 compares results obtained by our algorithm with the results reported in the literature.[1,8,9] The agreement is excellent for all inclination angles considered here and for all time ranges. This establishes the point that our algorithm presented in this paper is robust and accurate. We must also note that the computational times are favorable for the repeated evaluation of the solution as would be required by many other applications (such as regression) of the algorithm.

Table 1 presents wellbore responses of fully penetrating wells for $h_D=100$ and five values of the inclination angle, $\psi'=15$, 45, 75, 85, and 89°. Note that the case considered here is the same as that considered in Table 1 of Ref. 1 except that we may now compute pressures for inclination angles larger than 75°. Furthermore, the algorithm presented in this paper may also be used to accurately compute derivative responses. These computations are shown in **Table 2**.

In **Tables 3 through 7**, we present the dimensionless pressures of highly inclined, fully penetrating wells. This information is yet to be presented in the literature and supplements the tabular information presented by Cinco *et al.*[1] It can be observed from Tables 1 and 3 through 7 that the change in the pressure with respect to the inclination angle becomes larger as the inclination angle increases. As we show below, however, this is mainly a result of the accelerated increase in the well length as the inclination angle increases. Note that for fully penetrating wells, $h_{wD}=h_D/\cos\psi'$. For example, an increase in ψ' from 30 to 60° causes an increase in the well length by 1.73 times, whereas changing ψ' from 85 to 89° increases the well length by five times. Misinterpretation of this result sometimes causes the false expectation that the performance of a partially penetrating well can be considerably improved by simply increasing the slant angle.[2]

To demonstrate the potential of the algorithm presented in this paper, we also tabulate the pressure responses for two cases of partially penetrating, inclined wells. In **Tables 8 and 9**, the dimensionless formation thickness h_D is equal to 100 and 1,000, respectively. For Tables 8 and 9, the well length is equal to the formation thickness and the well is centrally located in the pay zone. The zero-inclination-angle case corresponds to a fully penetrating vertical well. Contrary to the observation we have made from Tables 1 and 3 through 7, here the influence of the inclination angle is more pronounced at small inclinations. As the well approaches a horizontal orientation, the influence of the inclination angle becomes practically unimportant (for most cases, the difference in pressures for $\psi'=75°$ and 90° is negligibly small).

We now present some results in graphical form. First, we consider fully penetrating, inclined wells. **Figs. 3 and 4** show the pressure responses of inclined wells for two values of the formation thickness: $h_D=100$ and 1,000. Inclination angles considered in these figures range from 0 to 89°. As suggested by Ref. 8, for vertical wells, we plot pressure responses in terms of $p_{wD}h_{wD}/h_D$. This group makes the responses for all inclinations

TABLE 7– DIMENSIONLESS WELLBORE PRESSURES OF HIGHLY INCLINED, FULLY PENETRATING WELLS, h_D=5,000

	p_{wD}					
t_D	$\psi'=77°$	$\psi'=80°$	$\psi'=82°$	$\psi'=85°$	$\psi'=87°$	$\psi'=89°$
1×10	0.3526	0.2722	0.2181	0.1366	0.0820	0.0273
2×10	0.4292	0.3313	0.2655	0.1662	0.0998	0.0333
5×10	0.5315	0.4102	0.3287	0.2058	0.1235	0.0412
7×10	0.5692	0.4393	0.3520	0.2204	0.1323	0.0441
1×10^2	0.6093	0.4702	0.3768	0.2358	0.1416	0.0472
2×10^2	0.6873	0.5304	0.4250	0.2660	0.1596	0.0532
5×10^2	0.7904	0.6101	0.4890	0.3060	0.1836	0.0611
7×10^2	0.8282	0.6394	0.5124	0.3208	0.1924	0.0640
1×10^3	0.8682	0.6703	0.5373	0.3364	0.2018	0.0671
2×10^3	0.9461	0.7304	0.5855	0.3667	0.2201	0.0732
5×10^3	1.0491	0.8099	0.6491	0.4067	0.2443	0.0812
7×10^3	1.0870	0.8391	0.6725	0.4213	0.2531	0.0841
1×10^4	1.1271	0.8701	0.6973	0.4368	0.2624	0.0873
2×10^4	1.2051	0.9302	0.7456	0.4669	0.2805	0.0935
5×10^4	1.3081	1.0098	0.8093	0.5069	0.3044	0.1017
7×10^4	1.3460	1.0390	0.8328	0.5215	0.3132	0.1047
1×10^5	1.3861	1.0700	0.8579	0.5371	0.3225	0.1078
2×10^5	1.4641	1.1302	0.9059	0.5673	0.3407	0.1137
5×10^5	1.5735	1.2144	0.9732	0.6094	0.3659	0.1221
7×10^5	1.6190	1.2493	1.0011	0.6268	0.3764	0.1255
1×10^6	1.6720	1.2900	1.0336	0.6471	0.3886	0.1296
2×10^6	1.7888	1.3803	1.1058	0.6922	0.4156	0.1386
5×10^6	1.9602	1.5168	1.2164	0.7616	0.4572	0.1525
7×10^6	2.0269	1.5712	1.2613	0.7902	0.4744	0.1582
1×10^7	2.1021	1.6330	1.3129	0.8237	0.4946	0.1649
2×10^7	2.2723	1.7738	1.4320	0.9041	0.5436	0.1813
5×10^7	2.5641	2.0192	1.6418	1.0522	0.6390	0.2134
7×10^7	2.6909	2.1293	1.7372	1.1207	0.6852	0.2295
1×10^8	2.8352	2.2576	1.8501	1.2029	0.7416	0.2497
2×10^8	3.1383	2.5369	2.1037	1.3945	0.8753	0.3009
5×10^8	3.5682	2.9490	2.4941	1.7176	1.1107	0.4011
7×10^8	3.7309	3.1079	2.6481	1.8541	1.2167	0.4493
1×10^9	3.9050	3.2791	2.8155	2.0070	1.3409	0.5080

collapse at early times. (The scaling of the time axis by h_D^{-2} only shifts the responses in real time and does not affect the shapes of the pressure-response curves in Figs. 3 and 4. As we show later in **Fig. 5**, however, it allows us to present the derivative responses for all values of formation thickness in one plot.) Figs. 3 and 4 indicate, as discussed before, that the influence of the inclination angle becomes magnified at large angles because of the accelerated increase in the well length by the increase in the inclination angle.

To complete our discussion of fully penetrating, inclined-well responses, we also consider the derivative responses in Fig. 5. The dimensionless formation thickness h_D does not appear as a parameter of interest. We were able to collapse the derivative responses for all values of formation thickness by scaling the time axis by h_D^{-2}. Fig. 5 clearly shows the early-time radial flow and late-time radial flow periods as predicted by our asymptotic approximations. We note that the late-time, radial-flow period is delayed considerably as the inclination angle increases. This is especially important for design purposes as the early-time, radial-flow period may be masked by wellbore storage and the shape of the intermediate-time responses are not distinctive for large inclination angles. The results shown in Fig. 5 have not been reported in the literature.

We now consider partially penetrating, inclined wells. **Figs. 6 and 7** show the composite plots of the pressure and derivative responses of partially penetrating inclined wells for $h_D=100$ and 1,000, respectively. In Figs. 6 and 7, the well is located centrally in the pay zone and a range of inclination angles between 0 and 90° is considered. In Fig. 6, the well length is equal to the formation thickness and in Fig. 7, it is half the thickness of the formation. Although not clearly evident in Figs. 6 and 7, examination of the data (see also Tables 8 and 9) indicates that, as we discussed earlier, the effect of the inclination angle is more important at small inclinations. Comparing the results in Figs. 6 and 7, we may conclude that the effect of the inclination angle becomes insignificant for all inclination angles, particularly if the length of the well is small compared with the formation thickness. Figs. 6 and 7, however, show that the pressure responses are not very sensitive (on log-log coordinates) to the inclination angle.

We further examine the issue of the influence of well length and angle on **Fig. 8**. Here, we assume a dimensionless formation thickness of $h_D=1{,}000$ and the well is located in the middle of the pay zone. The inset in Fig. 8 labels the combinations of the well length and inclination angle considered here. We have both partially penetrating and fully penetrating wells in Fig. 8. In general, the results shown in Fig. 8 support our earlier observation that the well length is a more important variable than the inclination angle. For example, a 75° slanted well has nearly the same pressure drop as a fully penetrating, vertical well if the well lengths are the same (Cases 2 and 3). Increasing the slant angle further to 90° does not change this result (Case 4). On the other hand, if the well length is equal to half of the formation thickness (Case 1), then the pressure

TABLE 8– DIMENSIONLESS WELLBORE PRESSURES OF PARTIALLY PENETRATING WELLS, $h_D=100$, $h_{wD}=100$, and $z_{wD}=50$

	p_{wD}				
t_D	$\psi'=0°$	$\psi'=30°$	$\psi'=60°$	$\psi'=75°$	$\psi'=90°$
1×10	1.5682	1.5683	1.5681	1.5681	1.5681
2×10	1.9085	1.9092	1.9085	1.9085	1.9085
5×10	2.3630	2.3613	2.3593	2.3593	2.3593
7×10	2.5305	2.5296	2.5212	2.5212	2.5212
1×10^2	2.7083	2.6955	2.6881	2.6880	2.6880
2×10^2	3.0542	3.0240	2.9934	2.9933	2.9933
5×10^2	3.5120	3.4257	3.3621	3.3552	3.3538
7×10^2	3.6802	3.5804	3.4939	3.4803	3.4768
1×10^3	3.8585	3.7464	3.6358	3.6138	3.6074
2×10^3	4.2050	4.0786	3.9258	3.8897	3.8781
5×10^3	4.6631	4.5161	4.3415	4.2955	4.2802
7×10^3	4.8313	4.6816	4.5010	4.4530	4.4371
1×10^4	5.0096	4.8582	4.6727	4.6232	4.6066
2×10^4	5.3562	5.2024	5.0114	4.9599	4.9427
5×10^4	5.8143	5.6589	5.4647	5.4121	5.3945
7×10^4	5.9826	5.8269	5.6320	5.5792	5.5616
1×10^5	6.1609	6.0049	5.8097	5.7567	5.7389
2×10^5	6.5075	6.3513	6.1554	6.1023	6.0844
5×10^5	6.9656	6.8092	6.6131	6.5598	6.5419
7×10^5	7.1339	6.9774	6.7812	6.7279	6.7100
1×10^6	7.3122	7.1558	6.9595	6.9062	6.8883
2×10^6	7.6588	7.5023	7.3060	7.2526	7.2347
5×10^6	8.1169	7.9604	7.7641	7.7107	7.6928
7×10^6	8.2852	8.1287	7.9323	7.8789	7.8610
1×10^7	8.4635	8.3070	8.1106	8.0573	8.0394

TABLE 9– DIMENSIONLESS WELLBORE PRESSURES OF PARTIALLY PENETRATING WELLS, $h_D=1{,}000$, $h_{wD}=1{,}000$, and $z_{wD}=500$

	p_{wD}				
t_D	$\psi'=0°$	$\psi'=30°$	$\psi'=60°$	$\psi'=75°$	$\psi'=90°$
1×10	1.5682	1.5683	1.5687	1.5688	1.5689
2×10	1.9085	1.9087	1.9089	1.9090	1.9090
5×10	2.3630	2.3631	2.3634	2.3634	2.3634
7×10	2.5305	2.5306	2.5309	2.5309	2.5309
1×10^2	2.7083	2.7084	2.7087	2.7087	2.7088
2×10^2	3.0542	3.0544	3.0546	3.0547	3.0547
5×10^2	3.5120	3.5121	3.5124	3.5125	3.5125
7×10^2	3.6802	3.6803	3.6806	3.6806	3.6806
1×10^3	3.8585	3.8587	3.8589	3.8589	3.8589
2×10^3	4.2050	4.2057	4.2053	4.2054	4.2054
5×10^3	4.6631	4.6616	4.6598	4.6599	4.6599
7×10^3	4.8313	4.8010	4.8224	4.8224	4.8224
1×10^4	5.0096	4.9664	4.9898	4.9898	4.9898
2×10^4	5.3562	5.3265	5.2957	5.2956	5.2957
5×10^4	5.8143	5.7285	5.6647	5.6578	5.6564
7×10^4	5.9826	5.8839	5.7965	5.7829	5.7795
1×10^5	6.1609	6.0488	5.9384	5.9165	5.9101
2×10^5	6.5075	6.3811	6.2285	6.1924	6.1808
5×10^5	6.9656	6.8186	6.6443	6.5983	6.5830
7×10^5	7.1339	6.9840	6.8038	6.7558	6.7398
1×10^6	7.3122	7.1608	6.9754	6.9259	6.9094
2×10^6	7.6588	7.5050	7.3141	7.2627	7.2456
5×10^6	8.1169	7.9614	7.7674	7.7149	7.6973
7×10^6	8.2852	8.1294	7.9348	7.8820	7.8643
1×10^7	8.4635	8.3075	8.1124	8.0595	8.0417
2×10^7	8.8101	8.6538	8.4582	8.4051	8.3872
5×10^7	9.2682	9.1118	8.9158	8.8626	8.8447
7×10^7	9.4365	9.2800	9.0840	9.0307	9.0128
1×10^8	9.6148	9.4583	9.2622	9.2090	9.1911

drop of the inclined well is considerably higher than that of the fully penetrating, vertical well. Increasing the well length while keeping the inclination angle constant (Cases 1, 3, and 5 to 7), decreases the pressure drop significantly. Based on these and the additional data we have examined, we conclude that it is the relative length of the well with respect to the formation thickness, not the individual values of the formation thickness, well length, and the inclination angle, that makes the performance of the inclined well noticeably different from that of a vertical well. In other words, the skin because of partial penetration dominates the pseudoskin factor of inclined wells.

Fig. 8 also shows the effect of the well length and inclination angle on derivative responses of inclined wells. Again, the well length is the main variable affecting the derivative responses. As shown by Cases 2 to 4 in Fig. 8, for a given well length, small deviations from vertical can result in noticeable differences in derivative behavior. As the well inclines further toward a horizontal orientation (inclination angles larger than 75°), however, the differences become smaller and the derivative responses merge, for all practical purposes, to the limiting curve for the 90° inclination case (see Cases 3 and 4).

The results we have presented thus far only concern wells that are located in the middle of the pay zone. In **Fig. 9**, we investigate the influence of the eccentricity of the well on the pressure and derivative responses. Here, the dimensionless formation thickness and well length are 5,000 and 1,000, respectively. Three well locations are considered: at the top of the formation [Case 1, $z_{wD}=h_D-(h_{wD}/2)\cos\psi'$], in the middle of the upper half of the pay zone (Case 2, $z_{wD}=3h_D/4$), and in the middle of the pay zone (Case 3, $z_{wD}=h_D/2$). For each location, a vertical well and a slanted well with 75° inclination are considered. It can be seen from Fig. 9 that the influence of the inclination angle becomes noticeable only when the well is adjacent to the top boundary

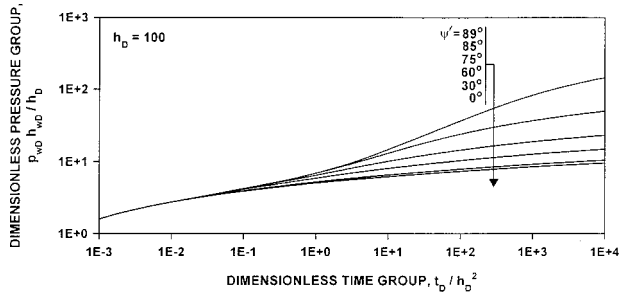

Fig. 3–Pressure responses of fully penetrating, inclined wells, $h_D=100$.

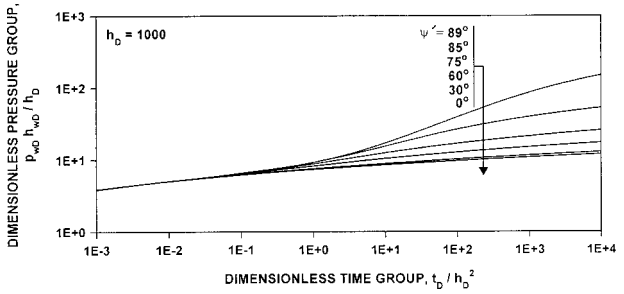

Fig. 4–Pressure responses of fully penetrating, inclined wells, $h_D=1{,}000$.

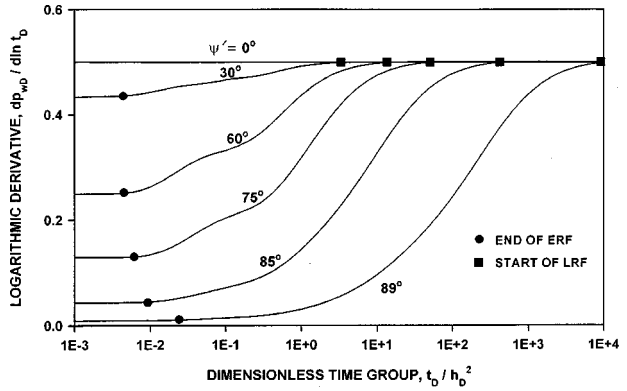

Fig. 5–Derivative responses of fully penetrating, inclined wells.

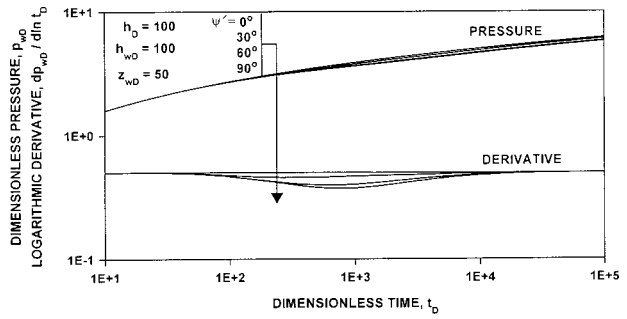

Fig. 6–Composite plot of partially penetrating, inclined-well responses, h_D=100, h_{wD}=100, and z_{wD}=50.

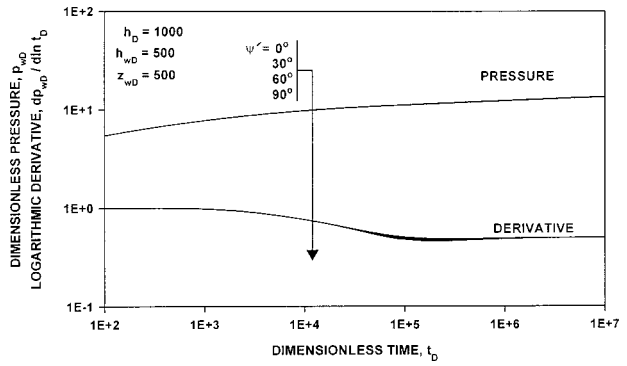

Fig. 7–Composite plot of partially penetrating, inclined-well responses, h_D=1,000, h_{wD}=500, and z_{wD}=500.

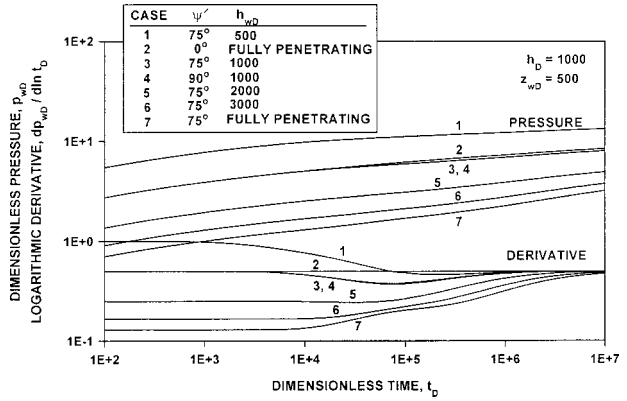

Fig. 8–Influence of length and angle on partially penetrating, inclined-well responses, h_D=1,000 and z_{wD}=500.

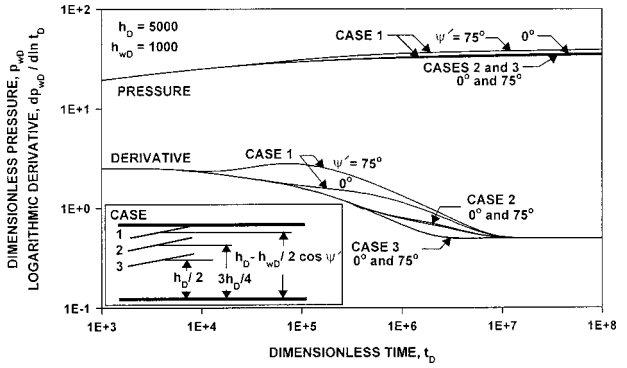

Fig. 9–Influence of eccentricity on partially penetrating, inclined-well responses, h_D=5,000 and h_{wD}=1,000.

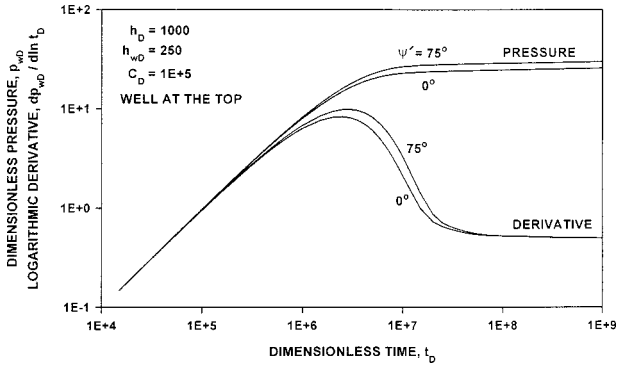

Fig. 10–Effect of wellbore storage on partially penetrating, inclined-well responses, h_D=1,000 and h_{wD}=250, well at the top.

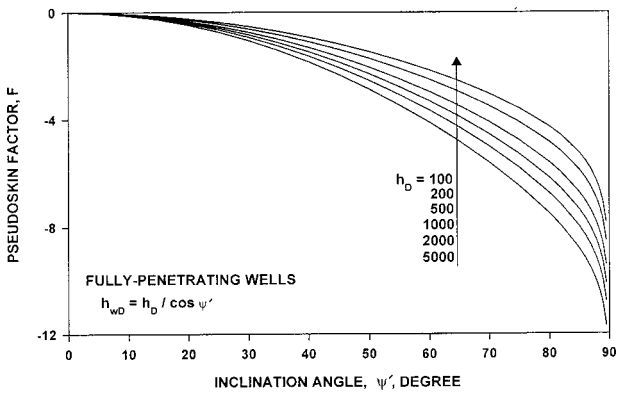

Fig. 11–Effect of inclination angle on pseudoskin factor of fully penetrating wells.

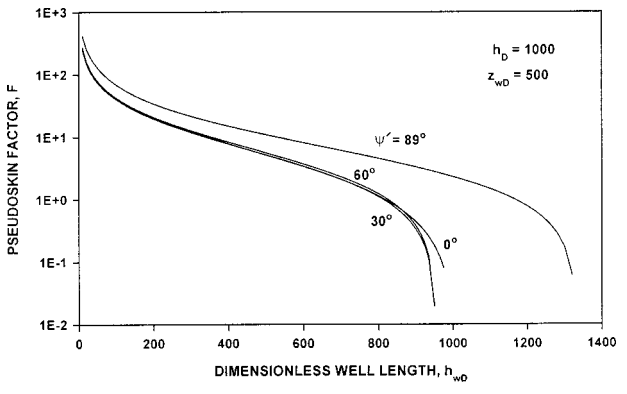

Fig. 12–Effect of inclination angle on pseudoskin factor of partially penetrating wells.

(Case 1). This indicates that the location of the well between the top and bottom boundaries of the formation becomes an issue only when the well is located closer to the boundaries. In other words, the pressure responses of inclined wells are not very sensitive to the location of the well. This conclusion is consistent with the findings of Ref. 9 for horizontal wells. Similar comments can be made about the influence of eccentricity on derivative responses.

As we noted before, one of the advantages of the algorithm we present in this paper is that the influence of wellbore storage may be readily incorporated. In **Fig. 10**, we intend to demonstrate this feature of our algorithm. Here, the dimensionless formation thickness is 1,000 and the dimensionless well length is 250. The well is adjacent to the top boundary. The dimensionless wellbore-storage constant C_D is defined in the conventional fashion and is chosen to be 10^5. Fig. 10 shows the pressure and derivative responses for $\psi' = 0°$ (vertical well) and 75° cases. Because our objective in Fig. 10 is to demonstrate the ability of our algorithm to incorporate the effect of wellbore storage, we do not comment on the characteristics of the responses. We, however, note that the case shown in Fig. 10 has been carefully chosen to display some effect of the inclination angle. In general, because a moderately large wellbore-storage coefficient masks the early- and intermediate-time flow periods, the influences of the formation thickness and well length will be more important for analyzing transient pressure and derivative responses of inclined wells.

We complete our discussion of results by considering the pseudoskin function of inclined wells. Here, we use the pseudoskin function expressions given in Eqs. 52 and 54. In **Fig. 11**, we present the pseudoskin factors of fully penetrating wells as a function of the inclination angle and formation thickness. As expected, the pseudoskin factor becomes more negative as the inclination angle and the formation thickness increases.

The pseudoskin factors shown in **Fig. 12** are for partially penetrating, inclined wells in a formation of dimensionless thickness 1,000. The midpoint of the well is located at the center of the pay thickness. All values of the pseudoskin factor are positive because for the well lengths considered here, for each inclination angle, the skin factor caused by partial penetration dominates the skin factor reflecting well inclination. Because of the complex interplay of the parameters involved, no general conclusion can be drawn (the curves for different inclinations can overlap, cross over, and terminate at different values). This requires that each case be evaluated specifically and makes the pseudoskin factor expression derived in this work extremely useful.

Concluding Remarks

The inclined-well solution and the expression for the pseudoskin function presented by Cinco *et al.*[1] have often been criticized because of their inability to incorporate the high-angle wells. This limitation has usually been attributed to the assumption of a line-source well and has led to the attempts to obtain pressure distributions around a well with a finite radius. Because of the growing popularity of the extended-reach and high-angle wells, many modifications to the Cinco *et al.* solutions have been attempted. In the process of development of a solution of general utility, however, many important considerations have been ignored. For example, at one end, Chen *et al.*[15] derived rigorously a surface-source solution in an attempt to remove the line-source-well limitation of the Cinco *et al.* model. They, however, failed to note that the region inside the surface source is filled with porous media and, as was noted by Gringarten and Ramey,[16] it is not an appropriate model to represent the finite-wellbore-radius case. At the other end, Fair *et al.*[2] developed a crude approximation to the inclined-well problem by assuming that a highly inclined well in a thin bed could be represented by a vertical fracture. As also noted in their work, the pseudoskin expression developed in Ref. 2 may only be a good approximation at the limit of vanishing formation thickness and near-horizontal well orientation. These works clearly show the desperate need for a well-grounded, rigorous expression to evaluate the performance of high-angle wells.

Starting with these motivating observations, we have accomplished three objectives in this work. First, we have developed rigorous expressions to compute the pressure responses and pseudoskin factors of inclined wells, including those of high inclinations. Second, we have shown that the limitation of the Cinco *et al.*[1] model regarding the high-angle wells is only computational. By reconstructing the solution in the Laplace domain and developing appropriate computational forms, this limitation has been removed in this work. Regarding the line-source-well assumption used in the derivations, it suffices to note that the justifications used for modeling vertical and horizontal wells as line sources are also valid for inclined wells. Our third contribution in this work is to document some results in tabular and graphical forms. This information should help those who develop their own codes by providing a reference. In addition, the discussions and the insight we provided should serve to better understand the inclined-well responses.

Nomenclature

a = defined by Eq. 21
b_i = defined by Eqs. 22–25
B = formation volume factor, bbl/stb
C = wellbore-storage coefficient, bbl/psi
c_t = total compressibility, psi^{-1}
e = defined by Eq. 26
$f(s)$ = naturally fractured reservoir function
F = defined by Eqs. 14, 18, and 20
$\hat{F}$ = defined by Eq. 44
$\hat{F}_a$ = defined by Eq. 47
$\hat{F}_b$ = defined by Eq. 48
F_1 = defined by Eqs. 15, 31, and 34
$\hat{F}_1$ = defined by Eq. 45
F_2 = defined by Eq. 16
$\hat{F}_2$ = defined by Eq. 46
h = formation thickness, ft
h_w = well length, ft
I = defined by Eq. 29
I_0 = defined by Eq. 49
k_h = permeability in horizontal direction, md
k_z = permeability in z direction, md
K_0 = modified Bessel function of the first kind of order 0
Ki_{1c} = defined in Eq. 28
l = reference length of the system, ft
p = pressure, psi
p_{Df} = defined by Eqs. 13, 17, and 19
q = production rate, stb/d
r = radial coordinate in horizontal plane, ft
r_w = wellbore radius, ft
R_D = defined by Eq. 9
s = Laplace transform parameter
S_g = pseudoskin factor
t = time, hours
u = defined in Eq. 10
u_n = defined in Eq. 11
x = x coordinate, ft
y = y coordinate, ft
z = distance in z direction, ft
z_{D1} = defined in Eq. 36
z_{D2} = defined in Eq. 37
z_w = location of well center in vertical direction, ft

Greek Symbols

α_n = defined by Eq. 27
β = defined by Eq. 41
ϵ_n = defined by Eq. 33
λ = defined by Eq. 35
ϕ = porosity
μ = viscosity, cp
π = 3.141 592 7
θ = coordinate from positive x direction, degrees
σ = defined by Eq. 40
ψ = inclination angle of the well, degrees

ψ' = transformed inclination angle (Eq. 7), degrees

Subscripts and Superscripts

D = dimensionless
i = initial
w = wellbore
$\bar{}$ = Laplace transform indicator

Acknowledgments

We thank Phillips Petroleum Co. for permission to present this paper.

References

1. Cinco, H., Miller, F.G., and Ramey, H.J. Jr.: ''Unsteady-State Pressure Distribution Created by a Directionally Drilled Well,'' *JPT* (November 1975) 1392; *Trans.*, AIME, **259**.
2. Fair, P.S., Kikani, J., and White, C.D.: ''Modeling High-Angle Wells in Laminated Pay Reservoirs,'' paper SPE 36027 presented at the 1996 SPE Annual Technical Conference and Exhibition, Denver, Colorado, 6–9 October.
3. Raghavan, R. and Ozkan, E.: *A Method for Computing Unsteady Flows in Porous Media*, Longman Scientific and Technical, Harlow, Essex, United Kingdom (1994) 41.
4. Lu, P.: ''Horizontal and Slanted Wells in Layered Reservoirs With Crossflow,'' MS thesis, Stanford U., Stanford, California (1997).
5. Ozkan, E. and Raghavan, R.: ''New Solutions for Well-Test-Analysis Problems: Part 2—Computational Considerations and Applications,'' *SPEFE* (September 1991) 369.
6. Kuchuk, F.J. and Kirwan, P.A.: ''New Skin and Wellbore Storage Type Curves for Partially Penetrated Wells.'' *SPEFE* (December 1987) 546.
7. Cinco, H.: ''Unsteady-State Pressure Distributions Created by a Slanted Well or a Well With an Inclined Fracture,'' PhD dissertation, Stanford U., Stanford, California (1974).
8. Gringarten, A.C. and Ramey, H.J. Jr.: ''An Approximate Infinite Conductivity Solution for a Partially Penetrating Line-Source Well,'' *SPEJ* (April 1975) 140; *Trans.*, AIME, **259**.
9. Ozkan, E., Raghavan, R., and Joshi, S.D.: ''Horizontal-Well Pressure Analysis,'' *SPEFE* (December 1989) 567; *Trans.*, AIME, **287**.
10. Cinco-Ley, H., Ramey, H.J. Jr., and Miller, F.G.: ''Pseudoskin Factors for Partially Penetrating, Directionally Drilled Wells,'' paper SPE 5589 presented at the 1975 SPE Annual Technical Conference and Exhibition, Dallas, 28 September–1 October.
11. Ozkan, E. *et al.*: ''Effect of Conductivity on Horizontal-Well Pressure Behavior,'' *SPE Advanced Technology Series* (March 1995) **3**, No. 1, 85.
12. Pucknell, J.K. and Clifford, P.J.: ''Calculation of Total Skin Factors,'' paper SPE 23100 presented at the 1991 SPE Offshore Europe Conference, Aberdeen, United Kingdom, 3–6 September.
13. Chen, G., Tehrani, D.H., and Peden, J.M.: ''Calculation of Well Productivity in a Reservoir Simulator,'' paper SPE 29121 presented at the 1995 SPE Symposium on Reservoir Simulation, San Antonio, Texas, 12–15 February.
14. Besson, J.: ''Performance of Slanted and Horizontal Wells on an Anisotropic Medium,'' paper SPE 20965 presented at the 1990 SPE Europec 90, The Hague, 22–24 October.
15. Chen, G., Tehrani, A.D.H., and Peden, J.M.: ''Pressure Distribution Created by a Slanted Well With Elliptic Inner Boundary Condition,'' paper presented at the Lerkendal Petroleum Engineering Workshop, Trondheim, Norway (1992).
16. Gringarten, A.C. and Ramey, H.J. Jr.: ''A Comparison of Different Solutions to the Radial Flow Problem,'' paper SPE 3817 available from SPE, Richardson, Texas (1972).

SI Metric Conversion Factors

bbl	×	1.589 873	E−01	= m^3
cp	×	1.0*	E−03	= Pa·s
ft	×	3.048*	E−01	= m
ft^3	×	2.831 685	E−02	= m^3
in.	×	2.54*	E+00	= cm
lbf	×	4.448 222	E+00	= N
lbm	×	4.535 924	E−01	= kg
psi	×	6.894 757	E+00	= kPa

*Conversion factors are exact.

SPEREE

Erdal Ozkan is an associate professor in the Dept. of Petroleum Engineering at the Colorado School of Mines in Golden, Colorado. e-mail: eozkan@mines.edu. He previously taught at Istanbul Technical U. Ozkan holds BS and MS degrees from Istanbul Technical U. and a PhD degree from the U. of Tulsa, all in petroleum engineering. He currently is a Review Chairman for *SPEREE*, and he served as the 1992–1993 Istanbul Technical U. Student Chapter faculty sponsor. **Rajagopal Raghavan** is a senior staff associate reservoir engineer at Phillips Petroleum Co. in Bartlesville, Oklahoma. e-mail: rara@ppco.com. He previously held positions on the faculties of the U. of Tulsa, Texas A&M U., and Stanford U., and at Amoco Production Co. Raghavan holds a BS degree in electrical engineering from the Birla Inst. of Technology, India, a diploma in petroleum production from the U. of Birmingham, England, and a PhD degree from Stanford U. A Distinguished Member and the recipient of the 1981 Distinguished Achievement for Petroleum Engineering Faculty and the 1988 Reservoir Engineering awards, he currently is the Senior Technical Editor of SPE. Raghavan has served on the Editorial Review Committee since 1980; he also has served as a member of the Books Committee (1994–1997), as a member (1988–1991) and Chairman (1991–1993) of the Symbols and Metrication Committee, as a member (1986–1988) and Chairman (1988–1989) of the Education and Accreditation Committee; as Chairman of several Forum Series in North America Steering Committees (1985–1986, 1988–1989, and 1998–1999); and as a member of Annual Meeting Technical Committees. Raghavan was a 1990–1991 SPE Distinguished Lecturer.